N-PENTANE CONVECTIVE BOILING HEAT TRANSFER INSIDE AN ANNULAR MICROCHANNEL

Evandro Rodrigo Dário, Gil Goss Júnior, Eduardo Victor Dias, Júlio César Passos

Departamento de Engenharia Mecânica, LEPTEN/Boiling, Universidade Federal de Santa Catarina, 88040-900 Florianópolis, SC, Brazil. E-mails: rdario@lepten.ufsc.br; goss@lepten.ufsc.br; eduardo.victor@lepten.ufsc.br; jpassos@emc.ufsc.br

ABSTRACT

An experimental study is here presented on heat transfer in the convective boiling of n-pentane, C_5H_{12}, in an annular microchannel, for input pressures and temperatures in the test section of 150 and 200 kPa, and 27 and 40°C, respectively. Mass velocity of up to 338 kg/m^{2}s for heat flux q" ≤ 60.0 kW/m^2 was employed. The test section is composed of two tubes, one inner copper tube where the heating is performed, and the other outer acrylic tube, mounted concentrically, with a gap between them of 0.25 mm, thus forming an annular minichannel with a hydraulic diameter of 0.5 mm. The effects of mass velocity, input pressure and temperature, and heat flux on the heat transfer coefficients for boiling were investigated. Experimental data for the heat transfer coefficients were compared with the correlations of Kandlikar (1990), Liu and Winterton (1991), Warrier (2002), Lazarek and Black (1982) and Steiner and Taborek (1992).

INTRODUCTION

The rapid development of industrial applications for micro-devices, micro-systems, advanced material design, and micro-manufacturing is creating a strong demand for a better understanding of micro-scale transport phenomena and is causing a notable shift in thermal science and heat transfer research from the macro- to micro-scale, as reported by Peng and Wang [1].

Boiling in microchannels and microstructures is an important topic in this area and has a particular significance in the development of new technologies and devices for control of energy transfer and other advanced applications requiring very compact and extremely large heat flux heat exchangers. The investigations of microscale transport processes conducted in the last decade have shown that microscale transport processes have distinct thermal fluid flow, heat transfer, and other thermal transport phenomena as compared to conventional situations, as was reported by Wen et. al. [2]. Experimental data in the literature also demonstrate that the boiling characteristics in microchannels can be different from those in macrochannels, although there isn't sufficient research available on the subject.

Thus, only part of the knowledge available on macroscale heat transfer can be transferred to the microscale, but it is not clear exactly what is still valid and what is not. In other words, there isn't yet a recognized transition threshold criterion from macroscale to microscale clearly defined for two-phase processes. Several classifications for this transition, based on the hydraulic diameter, D_h, for non-circular channels have been proposed.

Kandlikar [3] recommends the following classification and size ranges based on the D_h: microchannels (50–600 μm), minichannels (600 μm to 3 mm) and conventional channels (D_h > 3 mm). Such transition criteria are arbitrary and do not reflect the influence of the channel size on the physical mechanisms.

A better macro-to-micro transition criterion might be related to the bubble departure diameter. When the channel diameter is equal to or smaller than the capillary length, any additional increase in the bubble or caused by the coalescence of two or more bubbles will cause its deformation. In this case the confinement caused by the small space inside the channel will stretch the bubbles.

Kew and Cornwell [4] recommend using the confinement number, N_{CO}, as a criterion to differentiate between macroscale and microscale two-phase flow and heat transfer, defined according to Eq. (1):

$$N_{CO} = \left[\frac{\sigma}{g\left(\rho_g - \rho_g\right) D_h^{\,2}} \right]^{1/2} \qquad (1)$$

where σ, g, ρ_f and ρ_g represent the surface tension, the acceleration due to gravity, the liquid and the vapor density, respectively. The N_{CO} is equivalent to the ratio between the capillary length and the hydraulic diameter. These authors reported that the heat transfer and flow characteristics differed significantly to those observed in macrochannels for N_{Co} > 0.5. Hence, a second criterion for the transition between macro- and micro-scale, is adopted in this study:

- Microchannel - $N_{CO} > 0.5$
- Macrochannel - $N_{CO} < 0.5$

For n-pentane at atmospheric pressure, T_{sat} = 36°C, the capillary length for this criterion is 1.6 mm and becomes smaller as the saturation pressure increases.

Various investigators, such as Bowers and Mudawar [5], have recently demonstrated that the flow passage geometry has a significant impact on boiling, bubble generation and bubble growth in microchannels. The concept of 'evaporating space', as was reported by Peng and Wang [6], suggests that there is a minimum amount of space necessary to generate a vapor bubble in a confined microchannel. In fact, bubble size

has long been considered as a critical parameter in understanding the nucleate boiling characteristics and the dynamic bubble processes.

The objective of this study is to investigate the heat transfer in a forced flow boiling of n-pentane in an annulus microchannel, varying the mass velocity, heat flux, pressure, and subcooling at the entrance of the test section. The results for the boiling heat transfer coefficient, h_{tp}, will be compared with five different correlations developed for flow boiling in micro and macro (or conventional) channels. The tested correlations are listed in Tab. 2, in the Appendix.

EXPERIMENT

Experimental Apparatus

Figure 1 shows a schema of the experimental setup, which design and construction of the circuit of convective boiling and the test section were done at LEPTEN/Boiling. The working fluid is n-pentane, C_5H_{12}, and its properties are given in Tab. 1. The test loop consists of a magnetic gear pump; a pre-heater reservoir; a pre-heater, consisting of three tubes in line with a total length of 1.32 m; a mass flowmeter, a condenser and a reservoir.

The fluid temperature control in the pre-heater tubes is accomplished through type-E thermocouples inserted at their inlet and outlet, in the axis of the tube. The control of the power required for the heating is carried out automatically using the Labview software.

The mass flow rate is measured using a Coriolis flow meter with an uncertainty of ± 0.2 % in the reading. A valve, placed after the test section, controls the pressure during the experiment. Pressure is measured with two pressure transducers located at the entrance and exit of the test section.

The working fluid is cooled in the condenser, located after the test section. The cooling system uses water as the cold fluid. The water cooling system consists of a LAUDA RK20 KP cryostat.

Figure 2 shows a sketch of the test section, in an exploded view, which is composed of a copper tube with 29.9 mm diameter and 4.6 mm thickness. Inside this tube, seven type-E thermocouples were inserted with 0.3 mm diameter, located at the entrance, center and exit of the test section. The copper tube is heated by a cartridge-type electrical resistance inserted in its interior, which supplies the flow of heat imposed by the experiment. The copper tube is surrounded by a transparent acrylic tube, forming a mini channel which allows the visualization of the two-phase flow through it. To

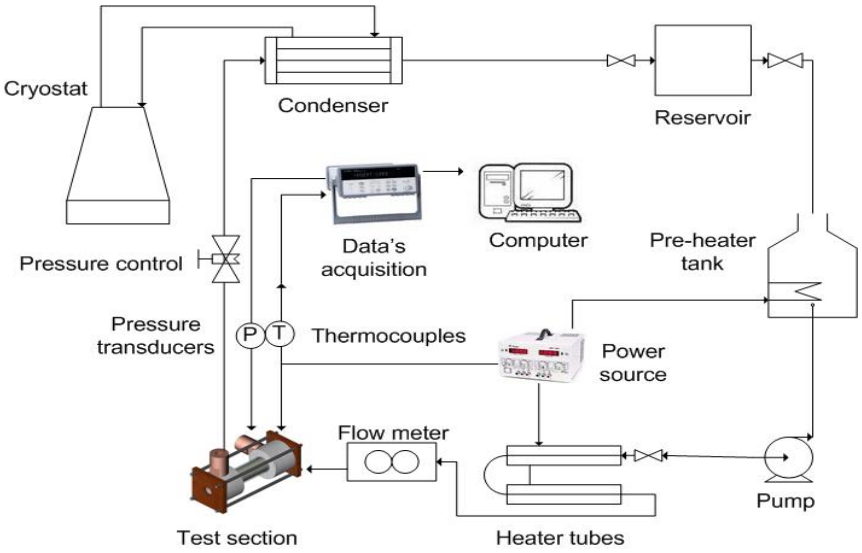

Figure 1 - Sketch of the experimental setup

In the reservoir pre-heater, located before the gear pump, the working fluid is heated up to a temperature close to the saturation temperature in order to eliminate gasses which could be dissolved in the fluid. This heating is accomplished by two cartridge-type resistors, inserted inside the reservoir. A relief valve, located at the top of the tank allows the elimination of gases to the outside. It also has a mixer to homogenize the temperature of the fluid in its interior.

By means of the gear pump, the mass flow rate is controlled during the two-phase flow tests in the range that could be tested, i.e., 40 to 400 kg/m^2 s.

The pre-heater tubes are used to maintain the working fluid at the desired temperature at the entrance of the test section. It is composed of three parallel steel tubes. The heat flux is accomplished through the Joule effect via a NiCr tape wound around the pre-heater tubes.

minimize the thermal losses to the atmosphere, the whole test section was insulated using glass wool.

The test section contains two plena, upstream and downstream of the micro channels, to ensure even flow distribution, as can be seen in Figure 2.

Two absolute pressures and two type-E thermocouple transducers are installed directly before the two plena to measure the inlet and outlet pressure and temperature.

The DC power supply is connected to the electrical resistor and controlled by a PC using Labview software. The acquisition and previous data treatment are carried out with an HP34970A system.

The temperature uncertainty was ± 0.6ºC.

Table 1 – Physical properties of n-Pentane at 100 kPa

Properties	**100 kPa (T_{sat}= 35.5ºC)**	
Molar mass, M_w	72.15	[kg/kmol]
Thermal diffusivity, α	7.953E-08	[m²/s]
Specific heat, c_p	2.363	[kJ/kgK]
Thermal condutibility, k	0.1136	[W/mK]
Kinematic viscosity, v	2.870E-07	[m²/s]
Viscosity, μ	1.735E-04	[kg /ms]
Latent heat of vaporization, h_{lv}	359.1	[kJ/kg]
Density of the líquid, ρ_l	604	[kg/m³]
Density of the vapor, ρ_v	2.89	[kg/m³]
Prandtl number of the líquid, Pr	3.609	
Surface Tension, σ	0.01432	[N/m]

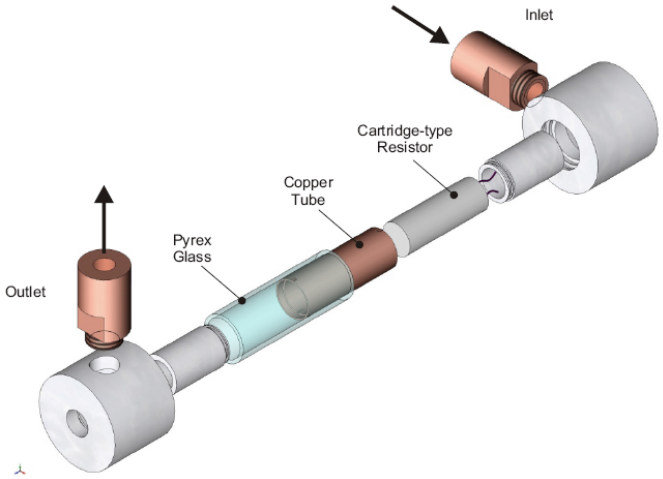

Figure 2 – Exploded view of test section

Experimental Procedure

Before the test begins, the reservoir is evacuated, passing all of the n-pentane to the reservoir pre-heater. Raising the temperature of the fluid to a temperature close to its saturation temperature forces the elimination of any gasses that would be dissolved, eliminating them to the atmosphere. The flow loop components are then adjusted to give the desired module inlet temperature, T_{in}, mass velocity, G, and inlet pressure, P_{in}, in test section.

When the desired conditions are reached, the test begins doing small increases in the heat flux at the test section. The conditions at the beginning of the test were maintained throughout the test.

The physical properties of n-pentane are presented in Tab. 1. For all test conditions, the working fluid was subcooled ($T_{in} < T_{sat}$) at the entrance of the test section.

The microchannels can therefore be divided into two regions: an upstream sub-cooled inlet region and a downstream saturated region; the location of zero thermodynamic equilibrium ($x_e = 0$) serves as a dividing point between the two regions. The length of the two regions can be evaluated using Eq. (2):

$$L_{sub} = \frac{\dot{m} c_{pl} \left(T_{sat,0} - T_{in}\right)}{q''_{ch} P_{wet}} \quad (2)$$

where $\dot{m}$ represents the mass flow, T_{sat} the saturation temperature of n-pentane at the location where x_e is zero, T_{in} the entrance temperature of the test section, P_{wet} the wetted perimeter, q''_{ch} is the heat flux imposed on the external surface of the copper tube, c_{pf} the liquid specific heat of n-pentane at T_{sat}, and L_{sub} the length of the sub-cooled area. Thereafter, L_{sat} is defined by Eq. (3).

$$L_{sat} = L - L_{sub} \quad (3)$$

where L and L_{sat} represent the length of the minichannel and the length of the two-phase flow regions, respectively.

The determination of the local flow boiling heat transfer coefficient requires knowledge of the local fluid temperature, microchannel wall temperature and heat flux. Since sub-cooled boiling may occur upstream of the point of zero thermodynamic equilibrium, the heat transfer coefficient can be accurately evaluated only at stream-wise locations which are in the saturate region ($x_e \geq 0$), and where the heat sink temperatures are measured by thermocouples. For the present test conditions, the two upstream thermocouples were mostly within the sub-cooled region. Therefore, only the saturated heat transfer coefficient results that were obtained at the center and outlet locations are of interest.

The saturation temperature, T_{sat}, is based on the local pressure. The pressure at the location of $x_e = 0$ can be considered very close to that measured at the channel inlet, P_{in}. Taking in account the value of the pressure measured at outlet of the channel, P_{out}, a linear interpolation was done to determine the pressure at the cross section where are istalled the wall thermocouples and then the saturation temperature T_{sat} was determined. This procedure for estimating the saturation temperature is based on the relatively small pressure drop (< 20 kPa) associated with this experiment. Once T_w, measured with thermocouples, and T_{sat} are determined, the value of mean flow boiling heat transfer coefficient, h_{tp}, can be determined from Eq. (4).

$$h_{tp} = \frac{(T_w - T_{sat})}{q''_{ch} A_t} \quad (4)$$

In the next section, the experimental results for n-pentane confined nucleate boiling in the mini channel will be presented and discussed for heat fluxes from 7.5 to 60 kW/m^2 and for mass flow rates of 85 to 338 kg/m^2 s.

The experimental uncertainly in the boiling heat transfer coefficient decreased with an increase in the heat flux. For 7.5 $< q''_{ch} <$20 kW/m^2 it was 9.0%, for 22.5 $< q''_{ch} <$40 kW/m^2 it was 6.9% and for 42.5 $< q''_{ch} <$60 kW/m^2 the experimental uncertainly was 6.2% of the h_{tp}.

Single-phase tests were firstly performed to determine the heat loss to the ambient and to validate the experimental apparatus and procedure. The rate of heat removal by the fluid can be measured by applying a macroscopic energy balance: $mc_{pl}(T_{out}-T_{in})$, and the measured power input is the product of the voltage and the current. The difference between the calculated heat removal rate and the measured power input was generally less than 3%.

RESULTS AND DISCUSSION

Figure 3 shows the behavior of the flow boiling heat transfer coefficient with the variation in the heat flux for different mass velocities (G), at the end of the test section. These data are obtained for inlet temperature and pressure of 40 ºC and 150 kPa, respectively, and show mass velocity values in the range of 85 – 170 kg/m^2 s.

It can be noted in Fig. 3 that the heat transfer coefficient is practically independent of the mass velocity, showing a small increase with the variation in the mass flux for $G \geq 254$ kg/m^2.s. this shows that the nucleate boiling has a greater influence on the heat transfer coefficient that convective boiling. Thus, the dominant mechanism in the heat transfer, in this study, is nucleate boiling. The h_{tp} increases with the heat flux increasing.

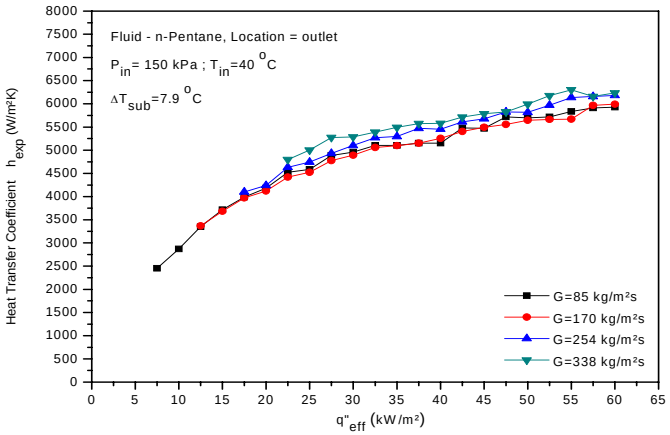

Figure 3 – Behavior of experimental data for heat transfer coefficiente versus q".

The experimental results for the local heat transfer coefficient, obtained with the experimental apparatus, described above, were compared with five empirical correlations, developed for flow boiling in microchannels and also for conventional channels, which are listed in Tab. 2.

For the comparison with the correlations, Bai et al. [7] proposed a different equivalent diameter when the channel has the annulus form, since there is non uniformity of the heating along the channel, because one of the surfaces is insulated. The equivalent heated diameter, for an annulus channel heated only on the inner face, is defined by Bai et al. [7] as:

$$D_{e,H} = \frac{4A_c}{P_H} = \frac{4\frac{\pi}{4}(d_o^2 - d_i^2)}{\pi d_i^2} = \frac{(d_o^2 - d_i^2)}{d_i} \qquad (5)$$

where d_o, d_i, A_c and P_H represent the outer and inner diameters, the cross sectional area and the heated perimeter of the annulus channel, respectively.

Figure 4 shows the experimental points and the predicted h_{tp} by the correlations for convective boiling. The experimental data increase with an increase in the vapor quality for all the qualities tested. For the experimental points the slope of the h_{tp}, however, lowers after x = 0.25. This change in the slope is not observed in the correlations proposed by Lazarek and Black [8] and Kandlikar [9]. The behavior of the Warrier et al. [12] correlation is very different.

In this case, the heat transfer coefficient decreases with an increase in the vapor quality up to x = 0.12, and then begins to increase.

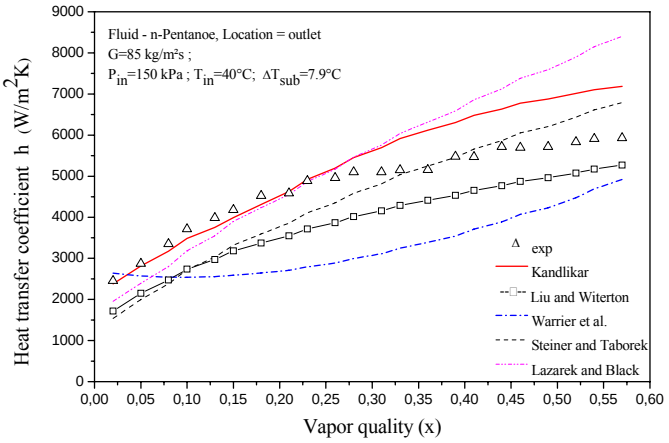

Figure 4 – Comparison with experimental data and correlations.

Comparisons between the correlations predicted and the experimental data obtained in this study are shown in Figs. 4 and 5(a) - (e). It's important to say that the correlations proposed by Lazarek and Black [8] and Warrier et al. [12] were developed for mini and microchannels. The three others tested correlations were developed for conventional channels.

The capability of each correlation to predict the experiments data is characterized by the mean absolute error (MAE), defined as:

$$MAE = \frac{100}{N}\sum_{n=1}^{N}\left|\frac{h_{tp,exp} - h_{tp,cor}}{h_{tp,exp}}\right| \qquad (6)$$

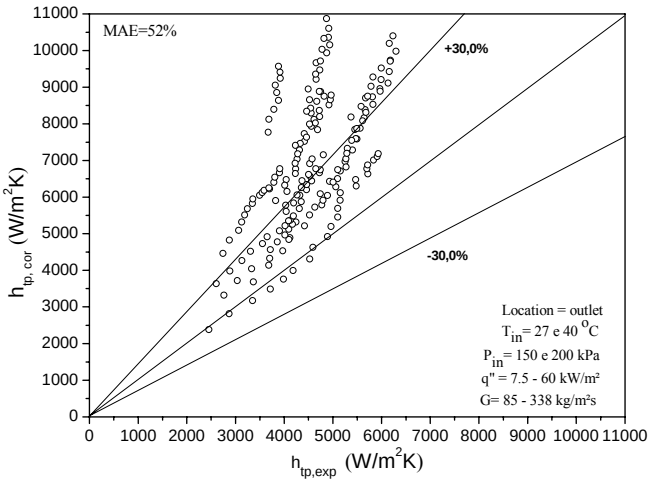

(a)

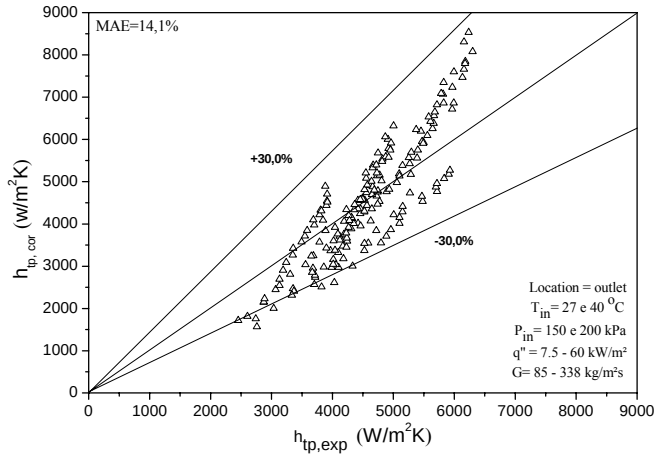

(b)

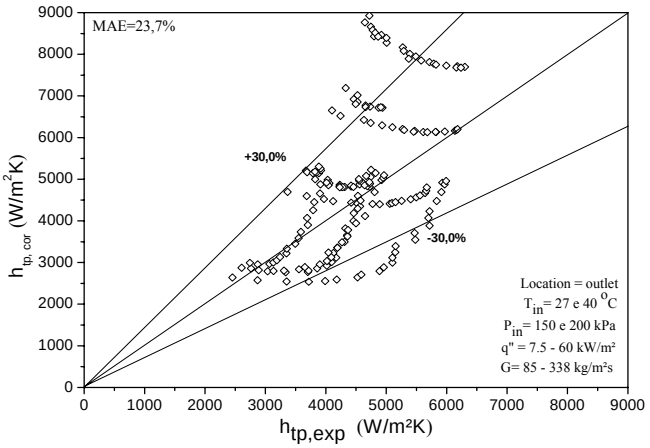

(c)

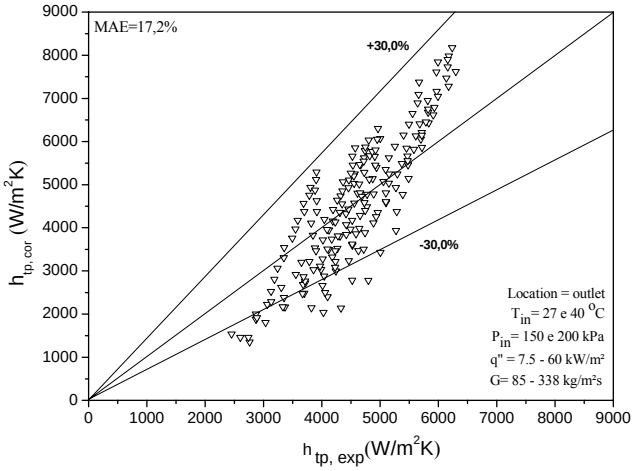

(d)

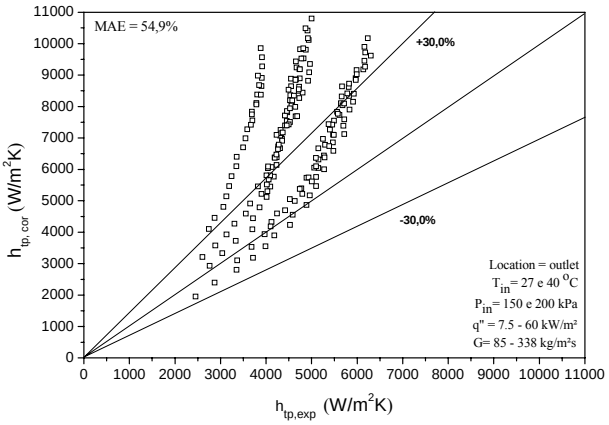

(e)

Figure 5 – Comparasion of two-phase heat transfer coefficient data with correlations of (a) Kandlikar [9], (b) Liu and Winterton [10], (c) Warrier et al. [12], (d) Steiner and Taborek [11], and (e) Lazarek and Black [8].

The best agreement between the experimental data and the correlations tested was obtained for the Liu and Winterton [10] correlation, with a MAE of 14.1%. The highest MAE was 54.9% for the Lazarek and Black [8] correlation. The other correlations had the followed MAE values: Steiner and Taborek [11] 17.2%, Warrier et al. [12] 23.7% and Kandlikar [9] 52%.

Sometimes, deviations between the correlation and the experimental data is due to the use of a different fluid and different ranges of test.

The results presented in this paper were obtained in the master dissertation of Dario [13].

CONCLUSIONS

This paper presented an investigation on the two phase heat transfer coefficient in an annular minichannel, with d_h = 0.5 mm, for n-pentane flow. The test conditions were: 85 < G < 338 kg/m^2 s; 0 < q" < 60 kW/m^2; inlet temperatures: 27 and 40 ºC; inlet pressure: 150 and 200 kPa.

The experimental data were compared with five correlations for the heat transfer coefficient in convective boiling. The summarized results are:

(i) The heat transfer coefficient is strongly dependent on the heat flux and is a weak function of the mass velocity. This indicates that the dominant heat transfer mechanism in this study was nucleate boiling.

(ii) The use of the equivalent heated diameter was a good approach to comparing the experimental data of an annulus minichannel with the correlations.

(iii) The correlations tested had a range of mean absolute error between 14.1% and 54.9%. The correlation that presented the smaller MAE was Liu and Winterton [10] correlation.

ACKNOWLEDGEMENTS

The authors are grateful for the support of CAPES and CNPq in the performance of this study. The experimental setup was financed by an EDITAL UNIVERSAL of CNPq.

NOMENCLATURE

Symbol	Quantity	SI
g	acceleration due to gravity	m/s^2
h	heat transfer coefficient	W/m^2K
h_{lv}	latent heat of vaporization	kJ/kg
L	length	m
q	heat flux	kW/m^2
T	temperature	K
N	number	-
D,d	diameter	m
$\dot{m}$	mass flux	kg/s
M_w	molar mass	kg/kmol
G	mass velocity	kg/m^2s
P	perimeter	m
c_p	specific heat	J/kgK
MAE	mean absolute error	-

Greek symbols

ΔT	wall superheating	K, °C
ρ	density	kg/m^3
σ	surface tension	N/m

Subscripts

l	liquid
lv	liquid-vapor
sat	saturation
v	vapor
w	wall
CO	confinement
sub	sub-cooled
i	inlet
o	outlet
h	hydraulic
ch	channel
tp	two-phase
cor	correlation
exp	experimental
wet	wetted
H	heated
E	equivalent
eff	effective

REFERENCES

[1] X F. Peng, B.X. Wang, Forced convection and boiling characteristics in microchannels, *Proceedings of the 11th International Heat Transfer*, vol. 1, Kyonji, Korea, 23–28 August, pp. 371–390, 1998.

[2] D.S. Wen, Youyou Yan and D.B.R. Kenning, Saturated flow boiling of water in a narrow channel: time-averaged heat transfer coefficients and correlations, Applied Thermal Engineering, vol. 24, Issues 8-9, pp. 1207-1223, 2004.

[3] S.G. Kandlikar, Fundamental issues related to flow boiling in minichannels and microchannels, Exp. Therm. Fluid Sci., vol. 26, pp. 389–407, 2002.

[4] P. Kew, K. Cornwell, Correlations for prediction of boiling heat transfer in small diameter channels. Applied Thermal Engineering, vol. 17, Issues 8–10, pp. 705–715, 1997.

[5] M.B. Bowers, and I. Mudawar, High flux boiling in low flow rate, low pressure drop mini-channel and microchannel heat sinks, International Journal of Heat and Mass Transfer, vol. 37, pp. 321-332, 1994.

[6] X.F. Peng and B.X. Wang, Forced-low convection and flow boiling heat transfer for liquid flowing through microchannels, International Journal of Heat and Mass Transfer, vol. 36, pp. 3421-3427, 1993.

[7] B.F. Bai, R. Huang, L.J. Guo, Z.J. Xiao, Physical model of critical heat flux with annular flow in annulus tubes, J. Eng. Thermophys, vol. 24, pp. 251–254, 2003.

[8] G.M. Lazarek, S.H. Black, Evaporative heat transfer, pressure drop and critical heat flux in a small vertical tube with R-113, International Journal of Heat and Mass Transfer, vol. 25, pp. 945–960, 1982.

[9] S.G. Kandlikar, A general correlation for saturated two-phase vertical tubes, Journal of Heat Transfer, vol. 112, pp. 219–228, 1990.

[10] Z. Liu, R.H.S. Winterton, A general correlation for saturated and subcooled flow boiling in tube and annuli, International Journal of Heat and Mass Transfer, vol. 34, pp. 2759–2766, 1991.

[11] D. Steiner, and J. Taborek, Flow boiling heat transfer in vertical tubes correlated by an asymptotic model, Heat Transfer Eng. , vol. 13, pp. 43–69, 1992.

[12] G.R. Warrier, V.K. Dhir, L.A. Momoda, Heat transfer and pressure drop in narrow rectangular channel, Exp. Therm. Fluid Sci., vol. 26, pp. 53–64, 2002.

[13] E.R.Dario, Convective boiling of n-Pentane inside an annular mini-channel, Master of Science Dissertation, Graduate Program of Mechanical Engineering, Federal University of Santa Catarina, 120 p., March, 2008.

APPENDIX

Table 2 – Flow Boiling heat transfer correlations

Reference	Heat transfer coefficient (h_{tp})
Lazarek and Black [8], 1982	$h_{tp} = 30\,\mathrm{Re}_{lo}^{0.857}\, Bo^{0.714}\, \frac{k_l}{D_h}$ $Bo = \frac{q_{eff}}{h_{lv} G}$
Kandlikar [9], 1990	$h_{tp} = MAX(E,S) h_{sp}$ $h_{sp} = 0.023 \left(\frac{k_l}{D_h} \right) \mathrm{Re}_{lo}^{0.8}\, \mathrm{Pr}_l^{0.4}$ $S = 1.1136 Co^{-0.9} f\left(Fr_l\right) + 667.2 Bo^{0.7}$ $E = 0.6683 Co^{-0.2} f\left(Fr_l\right) + 1058 Bo^{0.7}$ $Fr_l \geq 0.04 \rightarrow f\left(Fr_l\right) = 1 \quad Fr_l < 0.04 \rightarrow f\left(Fr_l\right) = \left(25 Fr_l\right)^{0.3}$ $Co = \left(\frac{1-x}{x} \right)^{0.8} \left(\frac{\rho_v}{\rho_l} \right)^{0.5}$
Liu and Winterton [10], 1991	$h_{tp} = \left[\left(E h_{sp}\right)^2 + \left(S h_{nb}\right)^2 \right]^{1/2}$ $h_{sp} = 0.023 \left(\frac{k_l}{D_h} \right) \mathrm{Re}_{lo}^{0.8}\, \mathrm{Pr}_l^{0.4}$ $E = \left[1 + x\, \mathrm{Pr}_l \left(\frac{\rho_l}{\rho_v} - 1 \right) \right]^{0.35}$ $h_{nb} = 55\, p_{red}^{0.12} \left(-\log_{10}\left(p_{red}\right) \right)^{-0.55} M_w^{-0.5} q_{eff}^{0.67}$ $S = \left(1 + 0.55 E^{0.1}\, \mathrm{Re}_{lo}^{0.16} \right)^{-1}$ $Fr_l = \frac{G^2}{g D_h \rho_l}$
Steiner and Taborek, [11], 1992	$h_{tp} = \left[\left(E h_{sp}\right)^3 + \left(S h_{nb}\right)^3 \right]^{1/3}$ $h_{sp} = 0.023 \left(\frac{k_l}{D_h} \right) \mathrm{Re}_{lo}^{0.8}\, \mathrm{Pr}_l^{0.4}$

Table 2 (Continued)

Reference	Heat transfer coefficient (h_{tp})
Steiner and Taborek, [11], 1992	$E = \left[\left(1-x\right)^{3/2} + 1.9x^{0.6}\left(\frac{\rho_l}{\rho_v}\right)^{0.35} \right]^{1.1}$ $S = F\left(\frac{q_{eff}}{1.5x10^5}\right)^{\left(0.8-0.1e^{1.75\,p_{red}}\right)}\left(\frac{0.01}{D_h}\right)^{0.4} f\left(M_w\right)$ $F = 2.816\,p_{red}{}^{0.45} + \left(3.4 + \frac{1.7}{1-p_{red}{}^7}\right)$ $f\left(M_w\right) = 0.72581;\ h_{nb} = 3010 W/m^2K$
Warrier et al. [12], 2002	$h_{tp} = Eh_{sp}$ $h_{sp} = 0.023\left(\frac{k_l}{D_h}\right)\mathrm{Re}_{lo}{}^{0.8}\,\mathrm{Pr}_l{}^{0.4}$ $E = 1 + 6Bo^{1/16} + f\left(Bo\right)x^{0.65}$ $f\left(Bo\right) = -5.3\left(1-855Bo\right)$